

AD-A182 203

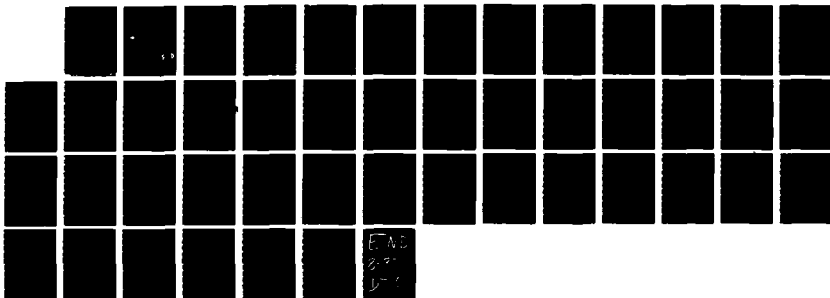
HEAVY METAL FLUORIDE GLASSES(U) HEBREW UNIV JERUSALEM
(ISRAEL) R REISFIELD ET AL APR 87 AFWL-TR-86-17
F29601-81-C-0012

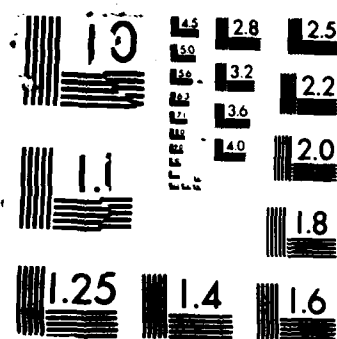
1/1

UNCLASSIFIED

F/G 11/2

NL





DTIC FILE COPY

②

AD-A182 203

HEAVY METAL FLUORIDE GLASSES

Professor Renata Reisfield
Dr Marek Eyal

The Hebrew University of Jerusalem
Jerusalem 910904 Israel

April 1987



Final Report

Approved for public release; distribution unlimited.

DTIC
ELECTE
JUN 26 1987
S D E

AIR FORCE WEAPONS LABORATORY
Air Force Systems Command
Kirtland Air Force Base, NM 87117-6008

87 6 23 078

This final report was prepared by The Hebrew University of Jerusalem, Jerusalem 910904 Israel, under Contract F29601-81-C-0012, Job Order ILIR8506, with the Air Force Weapons Laboratory, Kirtland Air Force Base, New Mexico. Diane J. Martin (ARBD) was the Laboratory Project Officer-in-Charge.

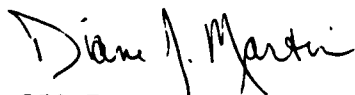
When Government drawings, specifications, or other data are used for any purpose other than in connection with a definitely Government-related procurement, the United States Government incurs no responsibility or any obligation whatsoever. The fact that the Government may have formulated or in any way supplied the said drawings, specifications, or other data, is not to be regarded by implication, or otherwise in any manner construed, as licensing the holder, or any other person or corporation; or as conveying any rights or permission to manufacture, use, or sell any patented invention that may in any way be related thereto.

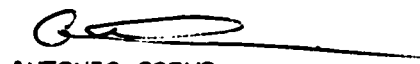
This report has been authored by a contractor of the United States Government. Accordingly, the United States Government retains a nonexclusive, royalty-free license to publish or reproduce the material contained herein, or allow others to do so, for the United States Government purposes.

This report has been reviewed by the Public Affairs Office and is releasable to the National Technical Information Services (NTIS). At NTIS, it will be available to the general public, including foreign nations.

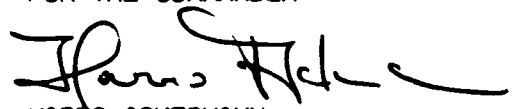
If your address has changed, if you wish to be removed from our mailing list, or if your organization no longer employs the addressee, please notify AFWL/ARBD, Kirtland AFB, NM 87117-6008 to help us maintain a current mailing list.

This technical report has been reviewed and is approved for publication.


DIANE J. MARTIN
Project Officer


ANTONIO CORVO,
Capt, USAF
Chief, Optical Components Branch

FOR THE COMMANDER


HARRO ACKERMANN
Lt Col, USAF
Chief, Laser Science and Technology

DO NOT RETURN COPIES OF THIS REPORT UNLESS CONTRACTUAL OBLIGATIONS OR NOTICE ON A SPECIFIC DOCUMENT REQUIRES THAT IT BE RETURNED.

6c. ADDRESS (City, State, and ZIP Code) Jerusalem 910904 Israel		7b. ADDRESS (City, State, and ZIP Code) Kirtland Air Force Base New Mexico 97117-6008	
8a. NAME OF FUNDING / SPONSORING ORGANIZATION	8b. OFFICE SYMBOL (If applicable)	9. PROCUREMENT INSTRUMENT IDENTIFICATION NUMBER F29601-81-C-0012	
8c. ADDRESS (City, State, and ZIP Code)		10. SOURCE OF FUNDING NUMBERS	
		PROGRAM ELEMENT NO. 61101F	PROJECT NO. ILIR
		TASK NO. 85	WORK UNIT ACCESSION NO. 06
11. TITLE (Include Security Classification) HEAVY METAL FLUORIDE GLASSES			
12. PERSONAL AUTHOR(S) Reisfield, Renata; and Eyal, Marek			
13a. TYPE OF REPORT Final	13b. TIME COVERED FROM 841221 to 860210	14. DATE OF REPORT (Year, Month, Day) 1987, April	15. PAGE COUNT 48
16. SUPPLEMENTARY NOTATION			
17. COSATI CODES		18. SUBJECT TERMS (Continue on reverse if necessary and identify by block number)	
FIELD	GROUP	SUB-GROUP	
11	04		
20	05		
		Fluorozirconate Glasses, Energy Transfer. Multiphonon Absorption. Laser Light Source,	

19. ABSTRACT (Continued)

doped fluoride glasses as light sources for fluoride fibers as an integral part of the fiber. (keywords) →

CONTENTS

<u>Section</u>	<u>Page</u>
1. INTRODUCTION	1
2. EXPERIMENTS	3
3. CHROMIUM(III) AND NICKEL(II) IN ZBLA GLASSES	5
4. NEODYMIUM(III) IN FLUORIDE GLASSES	11
4.1 <u>Steady state absorption and emission</u>	11
4.2 <u>Fluorescent lifetimes</u>	15
4.2.1 <u>Neodymium</u>	15
4.3 <u>Cross-relaxation</u>	17
5. ENERGY TRANSFER BETWEEN MANGANESE(II) AND NEODYMIUM(III)	22
5.1 <u>Manganese - steady state</u>	26
5.2 <u>Manganese lifetimes</u>	27
6. DISCUSSION	32
7. REVIEW	33
8. RECOMMENDATIONS	35
REFERENCES	36

Accession For	
NTIS GRA&I	<input checked="" type="checkbox"/>
DTIC TAB	<input type="checkbox"/>
Unannounced	<input type="checkbox"/>
Justification	
By _____	
Distribution/ _____	
Availability Codes	
Dist	Avail and/or Special
A-1	



ILLUSTRATIONS

<u>Figure</u>		<u>Page</u>
1	Absorption spectra of (a) Cr(III) and (b) Ni(II) at room temperature	5
2	Absorption spectrum of Nd(III) in sample d.	11
3	Emission spectrum of Nd(III) in PBLA glass.	15
4	Luminescence decay curves of Nd(III) in PBLA glass	19
5	Luminescence decay curves of Nd(III) in ZBLA glass	19
6	Scheme of energy levels of Nd(III) and Mn(II) in fluoride glass	22
7	Emission spectrum of Mn(II) in PBLA glass	23
8	Excitation spectra of Nd(III) in PBLA glass.	24
9	Absorption spectrum of Mn(II) in PBLA glass	28
10	Excitation and emission spectra of Mn(II) in PBLA and ZBLA glasses:	28
11	Luminescent decay curves of Mn(II) in PBLA and ZBLA glasses	30

TABLES

<u>Table</u>		<u>Page</u>
1	OPTICAL TRANSITIONS OF TRANSITION METAL IONS	6
2	LIFETIMES OF Nd(III) (876-nm EMISSION) AND Cr(III) (~800-nm EMISSION) IN ZBLA GLASS	8
3	OMEGA PARAMETERS IN ZBLA AND PBLA GLASSES	12
4	OSCILLATOR STRENGTHS AND LIFETIMES OF Nd(III) IN PBLA GLASS	14
5	NEODYMIUM IN PBLA GLASS	16
6	NEODYMIUM IN ZBLA GLASS [1 wt% Nd(III), 1 wt% Mn(III)]	16
7	CRITICAL RADII FOR CROSS-RELAXATION OF Nd(III) IN TELLURITE AND FLUORIDE GLASSES	18
8	SPECTROSCOPIC AND LASER PROPERTIES IN FLUORIDE GLASSES AS COMPARED TO OXIDE AND CHALCOGENIDE GLASSES	21
9	EFFICIENCY OF ENERGY TRANSFER FROM Mn(II) to Nd(III) IN PBLA GLASS	27
10	LIFETIMES OF Mn(II) IN ZBLA GLASS	29
11	LIFETIMES OF Mn(II) IN PBLA GLASS:	29

1. INTRODUCTION

Fluoride glasses containing about 50 mole% of ZrF_4 [which can be replaced by HfF_4 or ThF_4 (Refs. 1--3) or heavy metal fluorides based on PbF_2 and on 3d-group fluorides (Refs. 4, 5)] have been considered as materials for fiber optics in the range of 0.3--5 μm (Ref. 6).

The fluorozirconate glasses exhibit relatively low refractive indices in the visible range of about 1.5--1.59 and fairly good chemical resistance towards water and weak acids. Their mechanical properties still need to be improved and various methods of strengthening and protection are now being considered. These glasses have interesting optical properties which make them ideal candidates for producing optical fibers in the mid-infrared range (Refs. 7, 8). They represent an improvement over conventional silicate glasses for use in long-distance (above 100 km) repeaterless fiber links for transoceanic or transcontinental communications. One criterion for the high information bandwidth applications is the smallest possible second derivative $d^2n/d\lambda^2$ of the refractive index n ; this quantity actually vanishes for a wavelength λ_0 somewhere before the onset of the IR edge (Ref. 9).

Mixed fluorides are experimentally more difficult to prepare and handle and only a few cases of composition ranges remaining vitreous have been found and they tend to be much narrower than typical for mixed oxides. The first successful category of fluoride glasses was invented (Refs. 10, 11) at the University of Rennes, 1975, essentially consisting of zirconium(IV) and barium(II) fluoride and smaller amounts of fluorides of trivalent elements (colloquially called ZBLA glass). Another important category of fluoride glasses containing zinc(II) (or manganese), gallium(III) and lead(II) fluorides was invented (Ref. 4) at the University of Maine, Le Mans.

The absorption spectra and luminescence of $4f^{11}$ erbium(III) and $3d^5$ manganese(II), and the mutual energy transfer between excited states of these two species were studied in such a glass (Ref. 12). In ZBLA glass, the luminescence of $4f^2$ praseodymium(III) (Refs. 13, 14), $4f^6$ europium(III) (Refs. 15, 16), $4f^{10}$ holmium(III) (Refs. 17, 18) and erbium(III) (Refs. 19-21) occurs

from several more excited J-levels than usual because the lower limit (still allowing perceptible luminescence) for the energy gap between the emitting J-level and the closest lower-lying J-level is 2000 cm^{-1} (0.25 eV), some 2 to 4 times smaller than in nearly all other glasses and crystals. It may be noted that this rich emission spectrum (usually going down to several J-levels besides the ground state) is observed also at room temperature.

The superior optical characteristics of fluoride glasses for IR fiber optic applications also provide an ideal medium or host enabling the glass to be integrated into a system acting as a laser light source as well as the actual waveguide material. The spectroscopic and fluorescent properties of Nd(III) containing fluorozirconate glasses have been reported by Weber in work with the Lucas-Poulain group at Rennes (Ref. 10) and optical absorption of 3d transition metal ions such as Fe, Co, Ni and Cu by Ohishi et al (Ref. 22). Luminescence and nonradiative relaxation of rare earths in amorphous fluoride materials has recently been reviewed (Ref. 23).

The purpose of the present work is to investigate the absorption spectra of $3d^3$ [Cr(III)] and $3d^8$ [Ni(II)] in order to obtain information on site symmetry of a heavy metal in fluoride glass, to measure radiative transition probabilities, branching ratios, peak cross sections, lifetimes and laser threshold of rare earths exemplified by Nd(III) in order to determine laser properties of Nd(III) in fluoride glasses, and to look into energy transfer between Mn(II) and Nd(III) as a means of ameliorating the laser properties of Nd(III) in fluoride glasses.

2. EXPERIMENTS

The following doped glasses have been studied:

PBLA GLASS

- a. $36\text{PbF}_2, 24\text{MnF}_2, 35\text{GaF}_3, 2\text{AlF}_3, 3\text{YF}_3, 4\text{LaF}_3$
- b. $36\text{PbF}_2, 24\text{MnF}_2, 35\text{GaF}_3, 2\text{AlF}_3, 3.8\text{LaF}_3, 0.2\text{NdF}_3$
- c. $36\text{PbF}_2, 24\text{MnF}_2, 35\text{GaF}_3, 2\text{AlF}_3, 2\text{LaF}_3, 2\text{NdF}_3$
- d. $36\text{PbF}_2, 24\text{ZrF}_2, 35\text{GaF}_3, 2\text{AlF}_3, 3\text{YF}_3, 2\text{LaF}_3, 2\text{NdF}_3$

ZBLA GLASS

- e. $56.75\text{ZrF}_4, 34.25\text{BaF}_2, 4.5\text{LaF}_3, 4\text{AlF}_3, 0.5\text{CrF}_3$
- f. $56.50\text{ZrF}_4, 34.00\text{BaF}_2, 4.5\text{LaF}_3, 4\text{AlF}_3, 0.5\text{CrF}_3, 0.5\text{NdF}_3$
- g. $56.50\text{ZrF}_4, 34.00\text{BaF}_2, 4.5\text{LaF}_3, 4\text{AlF}_3, 0.5\text{CrF}_3, 0.5\text{MnF}_2$
- h. $55.75\text{ZrF}_4, 33.75\text{BaF}_2, 4.5\text{LaF}_3, 4\text{AlF}_3, 1\text{MnF}_2, 1\text{NdF}_3$
- i. $56.75\text{ZrF}_4, 34.25\text{BaF}_2, 4.5\text{LaF}_3, 4\text{AlF}_3, 0.5\text{NiF}_2$

The samples a,b,c,d were prepared as in Ref. 19 using metal fluorides as substrates. The samples a,b,c are slabs having square base of 7.85-mm, 6.75-mm and 8.1-mm edge length, respectively, and sample d is a rectangular slab of dimensions 2.5 x 8 x 12 mm. The samples of ZBLA glass (e,f,g,h,i) were prepared at La-Verre Fluore S.A.Z.I., Du Champ Martin, 35770 Vern-Sur-Seiche, France, and obtained from Dr B. Bendow, BDM Corporation, Albuquerque, NM, USA. The samples are 25 x 5 x 5 mm.

The absorption spectra were measured at room temperature on a Cary 14 and/or a Cary 219 spectrophotometer. Samples a,b,c were measured relative to air, and samples d,e,f,g,h,i were measured to undoped samples.

The emission and excitation spectra were measured on homemade spectrofluorimeters based either on a Spex monochromator or on a B&L monochromator (Ref. 19). Part of the spectra were corrected for the spectral response of the systems.

The decay curves of luminescence were obtained either by exciting the doped glasses with a Molelectron DL-200 tunable dye laser pumped by a Molelectron UV-400 pulsed nitrogen laser or by exciting the glass with the radiation of a nitrogen laser directly. The dyes used were as follows: Molelectron DPS (#4 with maximum of emission at 408 nm), Rhodamine 590 (#14) and 450 nm (#8 Dye). The transient signals were dispersed in a Jarrel-Ash monochromator (5-nm resolution) and detected by an R928 Hamamatsu photomultiplier. The amplified signals were captured at Biomation 8100 (10-ns resolution), stored in a Nicolet Analyzer and transferred to computer memory for further processing.

Since most of the decay curves analyzed in this study are nonexponential, the following definitions of integrated lifetime of luminescence were used:

$$\tau = \frac{\int I(t)tdt}{\int I(t)dt} \quad (1)$$

where $I(t)$ is the shape of the decay curve.

3. CHROMIUM(III) AND NICKEL(II) IN ZBLA GLASSES

Glass samples e and i were used for the absorption measurements. The absorption spectra of Cr(III) and Ni(II) at room temperature are given in Fig. 1. The observed band peaks, and ligand field and Racah parameters are presented in Table 1.

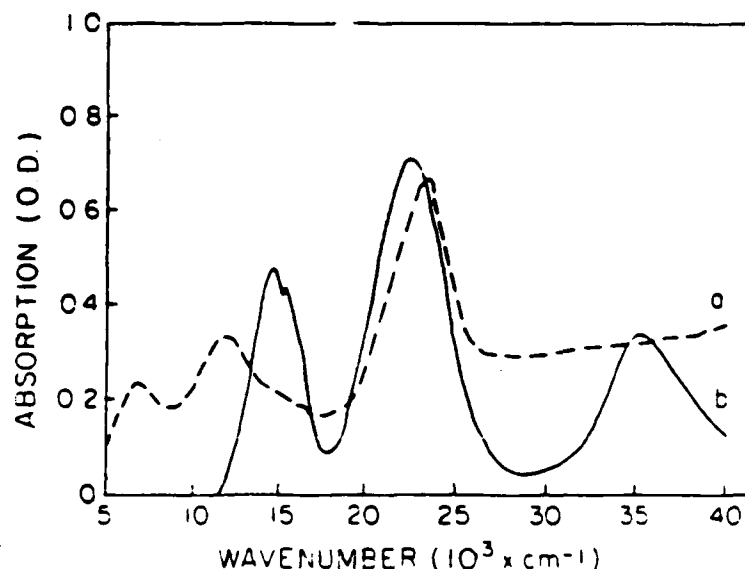


Figure 1. Absorption spectra of (a) Cr(III) and (b) Ni(II) at room temperature.

From the absorption spectra of Cr(III) and Ni(II) in ZBLA glass, both in this work and in that of Ohishi et al (Ref. 22), as well as from the absorption spectra of these ions in PBLA glass (Ref. 4), it can be demonstrated that the site symmetry for both Cr(III) and Ni(II) in these glasses is close to cubic octahedral symmetry. Sites of lower symmetry would have relatively much stronger absorption bands. Such a situation could be predicted for PBLA glass in view of the feasible substitution of Zn(II) and Ga(III) by Cr(III) of comparable radius.

Also, nearly all Cr(III) and a large majority of all paramagnetic Ni(II) complexes in solution, as well as solid compounds, show the coordination number $N = 6$ with octahedral symmetry. However, it is not perfectly trivial

TABLE 1. OPTICAL TRANSITIONS OF TRANSITION METAL IONS

ION	TRANSITION ASSIGNMENT	BAND POSITION		PARAMETERS	
		OBSERVED (cm ⁻¹)		(cm ⁻¹)	
		(Ref. 22)	(Ref. 31)	(Ref. 22)	(Ref. 31)
Cr(III)	⁴ A _{2g} (⁴ F) -- ⁴ T _{2g} (⁴ F)	14749	14800		
* *	⁴ A _{2g} (⁴ F) -- ² E _{1g} (² G)	15385	-	Dq = 1475	Dq = 1480
* *	⁴ A _{2g} (⁴ F) -- ⁴ F _{1g} (⁴ F)	22472	22500	B = 847	B = 850
* *	⁴ A _{2g} (⁴ F) -- ⁴ T _{1g} (⁴ P)	34483	34700	C = 3136	
Ni(II)	³ A _{2g} (³ F) -- ³ T _{2g} (³ F)	6536	6900		
* *	³ A _{2g} (³ F) -- ³ T _{1g} (³ F)	11364	11500	Dq = 663	Dq = 690
* *	³ A _{2g} (³ F) -- ³ E _{1g} (¹ D)	14925	-	B = 956	B = 970
* *	³ A _{2g} (³ F) -- ³ T _{1g} (³ P)	22936	23300	C = 4006	

Nephelauxetic parameter β in ZBLA glass (Ref. 31) is 0.926 for Cr(III) and 0.932 for Ni(II).

that Cr(III) and Ni(II) in ZBLA glass (known for Raman spectra (Ref. 24) to have more complicated coordination behavior) turn out to be octahedral to a high approximation. The subshell energy difference dq (also designated as Δ) corresponds to the maximum (or strictly to the center of gravity) of the first spin-allowed transition. The Racah parameter (Refs. 25, 26) of interelectronic repulsion B is derived from the diagonal sum rule

$$B = (\sigma_2 + \sigma_3 - 3\sigma_1)/15 \quad (2)$$

Such a derivation is rarely possible in Cr(III) because the third spin-allowed transition is usually hidden by electron transfer bands or other intense absorption. In such Cr(III) cases, B can be derived (Ref. 27) from σ_1 and σ_2 alone, providing $B = 875 \text{ cm}^{-1}$ for our sample. The nephelauxetic ratio β is the ratio between B from Eq. 2 and B_0 for the gaseous ion, 918 cm^{-1} for Cr^{+3} and 1041 cm^{-1} for Ni^{+2} . It is interesting to compare the parameters of Table 1 with related materials (vitreous and crystalline oxides) which were compiled for 36 Cr(III) cases (Ref. 28).

The value for dq of Cr(III) in ZBLA glass is distinctly lower than 16100 cm^{-1} reported (Ref. 29) for the cubic elpasolites $\text{K}_2\text{NaGa}_{0.95}\text{Cr}_{0.05}\text{F}_6$ and K_2NaCrF_6 suggesting 1.5 percent (0.03 Å) longer average Cr-F distances in the glass than in the crystal, as discussed below for analogous Ni(II) cases. The parameters in Table 1 are closer to CrF_6^{3-} in solution (Ref. 25) having $dq = 15200\text{ cm}^{-1}$ and $B = 820\text{ cm}^{-1}$ according to Claus Shaffer. They fall inside the intervals $dq = 14500$ to 16400 cm^{-1} and $B = 620$ to 850 cm^{-1} given (Ref. 30) for Cr(III) in 14 highly different mixed oxide glasses, and may also be compared with $dq = 17450$ and $B = 725\text{ cm}^{-1}$ for $\text{Cr}(\text{OH}_2)_6^{+3}$. The first absorption band of the fluorides and many oxide cases shows a complicated structure because the first two doublet levels 2E and 2T_1 almost coincide with 4T_2 , providing additional complications of spin-orbit coupling. The most prominent narrow peak occurs at 654 nm (15300 cm^{-1}) in our ZBLA glass, to be compared with 15430 cm^{-1} in a zirconium barium thorium fluoride glass (Ref. 30), which should represent the position of 2E to a good approximation.

Since 4T_2 stretches distinctly well below 2E , one expects any luminescence to be a broad-band transition between the two lowest quartet levels. Only very weak fluorescence of Cr(III) was seen in fluorophosphate glass (Ref. 30) and in ZBLA (Ref. 31). Lifetimes as well as the peak emissions of Cr(III) in ZBLA glass are presented in Table 2. The short lifetimes form a striking contrast, not only to the cubic elpasolites (Ref. 29) with temperature-dependent lifetimes in the range 0.2 to 0.6 ms, but also to Cr(III) in a lithium lanthanum phosphate glass (Ref. 32) with lifetimes around 0.02 ms (0.025 ms at the same low Cr(III) concentration as in the ZBLA glass) and a quantum yield up to 0.23. Much higher quantum yields are observed in glass-ceramics containing crystallites (much smaller than 400 nm) of spinel-type $\text{MgAl}_{2-x}\text{Cr}_x\text{O}_4$ and the izotypic gahnite $\text{ZrAl}_{2-x}\text{Cr}_x\text{O}_4$ (Ref. 33) and other types (Ref. 28, 34, 35). Such glass-ceramics may be useful as laser materials, conceivably replacing the crystalline alexandrite $\text{Al}_{2-x}\text{Cr}_x\text{BeO}_4$.

TABLE 2. LIFETIMES OF Nd(III) (876-nm EMISSION) AND Cr(III) (~800-nm EMISSION) IN ZBLA GLASS

DOPANT 1	DOPANT 2	EXCITATION λ , (nm)	EMISSION λ , (nm)	DECAY, (μ s)		
				τ_1	τ_2	τ_3
—	0.5 Cr	465	797	1.4	3.0	6.0
0.5 Mn	0.5 Cr	414	790	0.4	1.0	3.1
0.5 Nd	0.5 Cr	337	804	0.6	1.2	3.1
0.5 Mn	0.5 Cr	337	804	0.5	1.9	3.9
0.5 Nd	0.5 Cr	450	876	381	410	410
0.5 Nd	0.5 Cr	579	876	380	405	—

An attempt to record the steady-state emission of Cr(III) failed since the emission signal was of the order of the noise. Its lifetime, however, has been measured in the laser-induced luminescence experiments (Table 2).

The emission is most intense at 797 nm. It is noted that the nonexponential decay of the luminescence is quite common in glasses (Ref. 36). Here, however, the lifetimes are relatively short.

The dq value for nickel(II) in ZBLA glass is unusually small when compared with 8800 NiO; 8650 $\text{Ni}_x\text{Mg}_{1-x}\text{O}$; 8500 $\text{Ni}(\text{OH}_2)_6^{+2}$; 7400 NiTiO_3 ; and 7300 $\text{Ni}_x\text{Mn}_{1-x}\text{TiO}_3$ (all values in cm^{-1} (Ref. 25)). It is particularly interesting to compare with crystalline fluorides (Refs. 25, 37) such as 7800 spinel-type Li_2NiF_4 ; 7700 rutile-type NiF_2 ; 7500 perovskite-type KNiF_3 ($B = 950$ and 960 cm^{-1} in the two latter compounds to be compared with 940 cm^{-1} in $\text{Ni}(\text{OH}_2)_6^{+2}$ and 840 cm^{-1} in $\text{Ni}_x\text{Mg}_{1-x}\text{TiO}_3$). Rudorff, Kandler and Babel (Ref. 37) pointed out that such variations can be ascribed to slightly varying internuclear distances R . At face value one might consider a proportionality to R^{-5} as confirming the electrostatic model based on the tiny nonspherical part of the huge Madelung potential (this explanation is already beyond rescue because of the higher dq of water than of many oxygen-ligated anions) but Smith (Ref. 38) pointed out that an exponential variation $\exp(-kR)$ of the squares of the

overlap integrals (Refs. 39--41) entering the angular overlap model (Ref. 26) agrees with 5 percent increase of the antibonding effect for each percent decrease of R . In this perspective, ZBLA seems to have Ni-F distances on the average 1.6% (0.03 Å) longer than crystalline KNiF_3 . In mixed oxides more dramatic effects can occur, dq of Ni(II) being decreased to 6000 cm^{-1} in ilmenite-type $\text{Ni}_x\text{Cd}_{1-x}\text{TiO}_3$ (isomorphic with NiTiO_3 and MgTiO_3) and, as shown by Reinen, to only 4800 cm^{-1} in the perovskite (elpasolite superstructure?) $\text{Ba}_2\text{Ca}_{1-x}\text{TeNi}_x\text{O}_6$ (Ref. 25). However, in such substituted crystals (as in the classical case of ruby $\text{Cr}_x\text{Al}_{2-x}\text{O}_3$), a weak doubt always remains whether the distance $M-X$ between M carrying a partly filled shell and the closest neighbor atoms X fully adapts to the internuclear distances in the closed-shell host lattices. More convincing evidence comes from the hydrostatic high pressure (especially for atoms (Ref. 38) on special positions), but substituted crystals remain the only technique of significantly increasing R . A direct determination of R (with a precision of about 0.02 Å) is accessible to EXAFS using the X-ray absorption edge of the substituting M even in low concentration (Ref. 42).

The only possibility of luminescence of Ni(II) in ZBLA glass would be at the foot (some 6000 cm^{-1}) of the first absorption band, but we did not detect any. The spin-forbidden absorption band due to the first singlet level 1E corresponds to the rather broad shoulder at 15000 cm^{-1} (see Fig. 1) comparable to the peak (Ref. 37) of crystalline Ni(II) fluorides between 15000 and 15400 cm^{-1} .

As described in the experimental section, we also studied Nd(III) in ZBLA glass together with Mn(II) or Cr(III). Besides the well-known luminescence (Ref. 43) from $^4F_{3/2}$ situated 11400 cm^{-1} above the ground state, and seen to have the lifetime 0.34 ms when excited in the yellow to $^6G_{5/2}$ of Nd(III), short-lived (0.02 ms) emission is detected from $^2P_{3/2}$ (26100 cm^{-1} above the ground state and 2400 cm^{-1} above the closest lower J-level $^2D_{5/2}$) and a lifetime 1.5 μs from $^4D_{3/2}$ at 28100 cm^{-1} (2000 cm^{-1} above $^2P_{3/2}$).

In ZBLA glass simultaneously containing Nd(III) and Cr(III), energy transfer from Cr(III) by excitation in the strong absorption at 450 nm is

quite efficient, since the ${}^3F_{3/2}$ emission (to the Nd(III) ground state) at 876 nm has the same lifetime 0.4 ms as by excitation at 579 nm. This may be compared with the mutual influence (Ref. 32) between Cr(III) and Nd(III) in lithium lanthanum phosphate glass, where the lifetimes of one component alone in low concentration are in the 0.02-ms and 0.2-ms range respectively.

4. NEODYMIUM(III) IN FLUORIDE GLASSES

4.1 Steady-state absorption and emission

The absorption spectrum of neodymium in sample d is shown in Fig. 2. The spectrum serves as a basis for a complete set of predictions of transition rates within the $4f^3$ configuration of Nd(III). The procedure is based on the theory of Judd-Ofelt and is described in detail elsewhere (Refs. 19, 43). Here are described briefly the main steps of its evaluation.

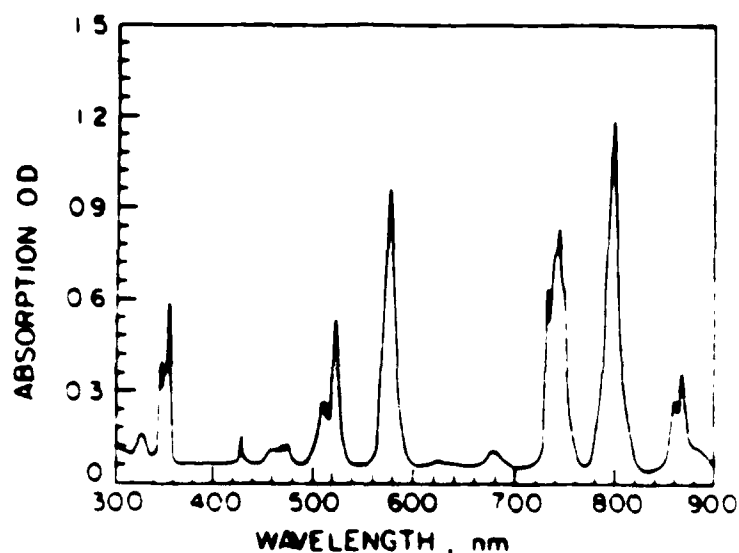


Figure 2. Absorption spectrum of Nd(III) in sample d.
(36PbF_2 , 24ZrF_2 , 35GaF_3 , 2AlF_3 , 3YF_3 , 2LaF_3 , 2NdF_3)

According to the theory the otherwise forbidden transitions within the $f-f$ configuration of rare-earths become slightly allowed by admixing of wave functions of the $f-f$ configuration with odd components of crystal field potential. The intraconfigurational transitions then become subject to a new set of selection rules, and oscillator strengths of the transitions depend parametrically on the three phenomenological parameters Ω_2 , Ω_4 , Ω_6 . Reduced matrix elements for the transitions are almost invariant in respect to the crystal field strength (Ref. 43) and were tabulated for all rare earth ions (Ref. 44).

The optical transitions of rare earths in solids are predominantly of electric dipole character and their spectral intensities can be described using the treatment of Judd and Ofelt. In this approach the line strength S of a transition between two J states is given by the sum of products of empirical intensity parameters Ω_t and matrix elements of tensor operators $U(t)$ of the form

$$S(J, J') = e^2 \sum_t \Omega_t | \langle aJ || U(t) || bJ' \rangle |^2 \quad (3)$$

where $t = 2, 4, 6$.

The values of Ω_t are obtained from a least-squares fit of measured and calculated absorption line strengths and typically have an experimental uncertainty of about 10 percent. The integrated intensities of the absorption bands yield Ω 's which are an effective average over the different rare earth environments in the glass. The most significant factor determining the values is the strengths of the odd-order terms in the expansion of the local field at the rare earth sites. These in turn are affected by the nearest-neighbor anion(s) and cations. For a given glass former systematic changes of Ω_t have been observed with the changes in the size and charge of network modifier ions (Ref. 45, 61).

The three omegas are determined by solving an overdetermined set of linear equations built by equating the measured oscillator strengths with the sum of products of the unknown omegas with the appropriate reduced matrix elements. The three omegas found from the solution are put into a computer program which calculates all the radiative transition rates possible in the system analyzed. The omega parameters for ZBLA and PBLA glasses are given in Table 3.

TABLE 3. OMEGA PARAMETERS IN ZBLA AND PBLA GLASSES

GLASS	REFERENCE	$\Omega_2, [\text{pm}^2]$	$\Omega_4, [\text{pm}^2]$	$\Omega_6, [\text{pm}^2]$
PBLA	31	1.01 ± 0.28	3.73 ± 0.35	6.19 ± 0.43
ZBLA	31	1.10 ± 0.25	3.80 ± 0.30	5.53 ± 0.20
ZBLA	10	1.95 ± 0.26	3.65 ± 0.38	4.17 ± 0.17

The next step is the calculation of nonradiative transfer rates due to multiphonon decay (Ref. 46). This is done by (1) subtracting the calculated radiative rates from the reciprocals of the integrated lifetimes of as many energy levels of the rare earth ions as possible, and (2) plotting the logarithms of the numbers against energy gaps between the levels and their nearest lower neighbor. Then the two parameters of an exponential multiphonon decay rate law are calculated: the exponential parameter α from the slope of the plot and the electronic factor B from its intercept.

Since only three energy levels of Nd(III) in our samples have lifetimes long enough to be measurable by our apparatus, the α and B were determined from 3 points only. The result, which is $\alpha = 0.0053 \pm 0.0005$ and $B = 1.63 \pm 0.1 \times 10^{10}$, agrees well with other sets of data which were measured on Ho(III) in ZBLA glass in our laboratory (Ref. 13). The parameters are inserted into

$$W_{nr} = B \exp[-\alpha \Delta E] \quad (4)$$

where ΔE is the energy gap from the emitting electronic level to its next lower neighbor. The entire set of transition rates is calculated, now with the nonradiative transition rates included (Ref. 46).

The result of such a procedure is shown in Table 4. The calculated oscillator strengths agree well with the measured values and the ω calculated from our ZBLA glass compare well with the values obtained by Lucas et al (Ref. 10) in their study of Nd(III) in ZBLA glass.

The last two columns in Table 4 compare calculated lifetimes with measured integrated lifetimes. The outstanding property of fluoride glasses is the relatively long-lived luminescence from levels which are separated only by a small energy gap to the next lower level (Ref. 18). Here one can record (see Fig. 3) and measure the lifetime of emission from two levels: ${}^4D_{3/2}$ (361 nm) and ${}^2P_{3/2}$ (387 nm). The first three emission lines seen in Fig. 3 are identified as belonging to the following transitions: ${}^4D_{3/2} - {}^4I_{9/2}$ (361 nm), ${}^4D_{3/2} - {}^4I_{11/2}$ (381 nm) and ${}^4D_{3/2} - {}^4I_{13/2}$ (412 nm). The next, much weaker group of lines belongs mainly to the transitions from ${}^2P_{3/2}$. The oscillator

TABLE 4. OSCILLATOR STRENGTHS AND LIFETIMES OF Nd(III)
IN PBLA GLASS: SAMPLE (d)

TRANSITION	WAVELENGTH (nm)	OSCILLATOR STRENGTHS		LIFETIMES, (μ s)	
		OBSERVED	CALCULATED	τ_{int}	CALCULATED
$^4D_{1/2}-^4I_{9/2}$	354}	9.04	4.27	--	0.00007
$^4D_{5/2}-^4I_{9/2}$	357}	9.04	1.27	--	0.00009
$^4D_{3/2}-^4I_{9/2}$	361	--	3.7	1.5	1.0
$^4D_{3/2}-^4I_{11/2}$	381	--	11.5	1.4	1.0
$^4D_{3/2}-^4I_{13/2}$	412	--	1.15	1.2	1.0
$^4D_{3/2}-^4F_{5/2}$	637	--	5.10	1.70	1.0
$^2P_{3/2}-^4I_{9/2}$	387	0.09	0.05	--	13.6
$^2P_{3/2}-^4I_{11/2}$	419	--	1.00	19.0	13.6
$^2P_{3/2}-^4I_{13/2}$	454	0.04	0.04	15.0	13.6
$^2P_{3/2}-^4I_{15/2}$	502	--	0.01	18.0	13.6
$^2P_{3/2}-^4H_{9/2}$	746	--	2.40	18.0	13.6
$^2P_{3/2}-^4F_{9/2}$	886	--	2.40	18.5	13.6
$^2D_{5/2}-^4I_{9/2}$	426}	0.17	0.04	--	0.0008
$^2P_{1/2}-^4I_{9/2}$	427}	0.17	0.09	--	0.3000
$^4G_{11/2}-^4I_{9/2}$	475}	1.38	0.21	--	0.00003
$^4D_{3/2}-^4I_{9/2}$	478}	1.38	0.35	--	0.00005
$^4G_{9/2}-^4I_{9/2}$	483}	1.38	0.42	--	0.1000
$^4G_{9/2}-^4I_{9/2}$	510}	1.38	1.50	--	0.0002
$^4G_{7/2}-^4I_{9/2}$	523	6.98	2.70	--	0.2500
$^2G_{7/2}-^4I_{9/2}$	577}	9.78	2.74	--	0.00015
$^4G_{5/2}-^4I_{9/2}$	577}	9.78	7.30	--	0.0040
$^2H_{11/2}-^4I_{9/2}$	620	0.18	0.18	--	0.0200
$^4F_{9/2}-^4I_{9/2}$	678	0.37	0.66	--	0.0100
$^4F_{7/2}-^4I_{9/2}$	732}	6.41	5.70	--	0.00004
$^4S_{3/2}-^4I_{9/2}$	743}	6.41	0.03	--	0.0009
$^2H_{9/2}-^4I_{9/2}$	797}	7.13	1.40	--	0.00006
$^4F_{5/2}-^4I_{9/2}$	802}	7.13	6.20	--	0.0090
$^4F_{3/2}-^4I_{9/2}$	860	1.92	2.20	190.0	337.00
$^4F_{3/2}-^4I_{9/2}$	867	2.00	2.30	180.0	326.00 ^a
$^4F_{3/2}-^4I_{9/2}$	867	2.10	2.20	330.0	337.00 ^b

^aSample c (PBLA glass). Nd(III) excited at 579 nm.^bSample b (PBLA glass). Nd(III) excited at 579 nm.

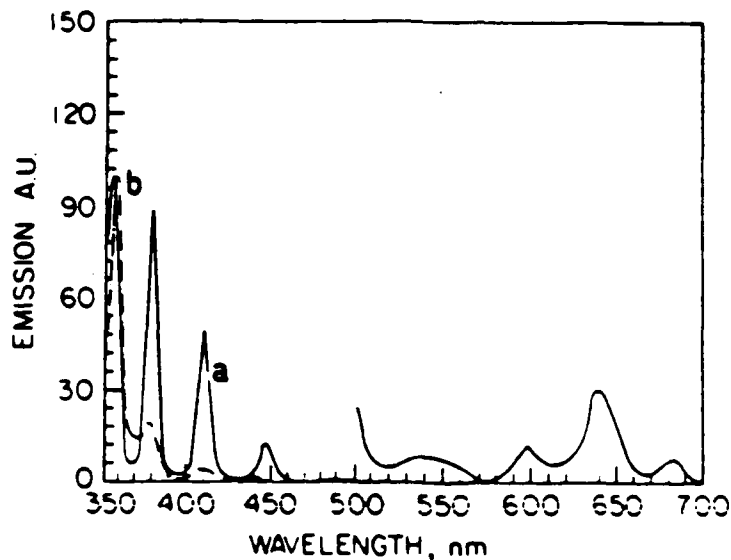


Figure 3. Emission spectrum of Nd(III) in PBLA glass. Excitation at 348 nm. (a) $36\text{PbF}_2, 24\text{ZrF}_2, 35\text{GaF}_3, 2\text{AlF}_3, 3\text{YF}_3, 2\text{LaF}_3, 2\text{NdF}_3$. The part of spectrum in 500--700nm is enlarged by a factor of 5 in respect to the intensity in 350--500nm region. (b) $36\text{PbF}_2, 24\text{MnF}_2, 35\text{GaF}_3, 2\text{AlF}_3, 2\text{LaF}_3, 2\text{NdF}_3$.

strengths of this group are an order of magnitude smaller than of the former group in accordance with the predicted values. These are the lines observed at 445 nm, 502 nm and the weak (not shown) lines at 746 nm and 886 nm (which are nevertheless easily recognized by their laser-induced emission). The lines at 637 nm originate from the $^4\text{D}_{3/2}$. The spectroscopic assignments of these lines are given in Tables 5 and 6.

4.2 Fluorescent lifetimes

4.2.1 Neodymium. Lifetimes of three energy levels of Nd(III) were measured from the laser-induced luminescence decays. Most of these emissions were observed also in the steady-state measurement.

The transitions which were too weak to be observed in the steady-state experiments were nevertheless observed and identified by wavelength and lifetime. The first group of transitions having lifetimes varying from 1.4 to 2.1 μs belongs to the transitions from the ^4D manifold. Its predicted lifetime is

TABLE 5. NEODYMIUM IN PBLA GLASS; $35\text{PbF}_2, 24\text{MnF}_2, 35\text{GaF}_3, \text{AlF}_3, (4-x)\text{LaF}_3, x\text{NdF}_3$

TRANSITION	X	WAVELENGTH (nm)		LIFETIMES (μs)				RISETIME	
		EXCITATION	EMISSION	τ_1	τ_2	τ_3	τ_{in}	SHORT	LONG
$^4\text{D}_{3/2} - ^4\text{I}_{9/2}$	0.2	337	360	1.4	1.5	1.8	1.5	<0.5	-
$^4\text{D}_{3/2} - ^4\text{I}_{11/2}$	0.2	337	381	1.8	2.0	2.3	2.0	<0.5	-
?	0.2	337	810	471	-	-	471	0.60	44
?	0.2	407	810	614	-	-	614	0.60	49
$^4\text{F}_{3/2} - ^4\text{I}_{9/2}$	0.2	337	865	567	507	499	500	1.5	70
$^4\text{F}_{3/2} - ^4\text{I}_{9/2}$	0.2	407	865	632	642	-	637	1.5	85
$^4\text{F}_{3/2} - ^4\text{I}_{9/2}$	0.2	579	865	265	327	345	330	-	7.0
$^4\text{D}_{3/2} - ^4\text{I}_{9/2}$	0.2	337	361	1.3	1.5	1.7	1.5	<0.5	-
$^4\text{D}_{3/2} - ^4\text{I}_{11/2}$	0.2	337	381	1.2	1.4	1.8	1.5	<0.5	-
$^2\text{P}_{3/2} - ^4\text{I}_{11/2}$	2.0	337	419	18.0	20.0	21.0	20.0	<0.5	1.5
$^2\text{P}_{3/2} - ^4\text{I}_{11/2}$	2.0	337	499	19.0	18.0	18.0	18.0	<0.5	1.5
$^4\text{D}_{3/2} - ^4\text{F}_{5/2}$	2.0	337	637	1.8	-	-	1.8	<0.5	-
$^2\text{P}_{3/2} - ^2\text{H}_{9/2}$	2.0	337	743	18.0	18.0	20.0	18.0	<0.5	1.5
$^4\text{F}_{3/2} - ^4\text{I}_{9/2}$	2.0	337	867	176	215	238	220	-	3.0
$^4\text{F}_{3/2} - ^4\text{I}_{9/2}$	2.0	407	867	180	210	240	220	-	3.0
$^4\text{F}_{3/2} - ^4\text{I}_{9/2}$	2.0	579	867	172	192	210	196	-	3.0
$^2\text{P}_{3/2} - ^4\text{F}_{9/2}$	2.0	337	886	18.0	24.0	28.0	25.0	<0.5	2.5

TABLE 6. NEODYMIUM IN ZBLA GLASS [1 wt% Nd(III), 1 wt% Mn(III)]

TRANSITION	WAVELENGTH (nm)		LIFETIMES (μs)				RISETIME (μs)
	EXCITATION	EMISSION	τ_1	τ_2	τ_3	τ_{in}	
$^2\text{P}_{3/2} - ^4\text{I}_{13/2}$	337	454	17.0	22.0	19.0	18.0	1.5
$^2\text{P}_{3/2} - ^4\text{I}_{15/2}$	337	499	24.0	27.0	31.0	26.0	3.0
$^4\text{D}_{3/2} - ^4\text{F}_{5/2}$	337	637	1.1	1.4	1.6	1.5	-
?	337	810	614	-	-	614	125
$^4\text{F}_{3/2} - ^4\text{I}_{9/2}$	337	876	533	560	604	570	80
$^4\text{F}_{3/2} - ^4\text{I}_{9/2}$	400	876	1045	1590	1500	1450	185
$^4\text{F}_{3/2} - ^4\text{I}_{9/2}$	579	876	320	330	350	340	1.5

0.97 μ s. The second group of lifetimes (15--20 μ s) belongs to the transitions from $^2P_{3/2}$. Its predicted lifetime is 13.6 μ s. The predictions based on the Judd-Ofelt combined with the exponential multiphonon law are not expected to give a better agreement (Ref. 13).

The lifetime of $^4F_{3/2}$ level is 190 μ s in sample d [2 wt% Nd(III)], 330 μ s in sample b [0.2 wt% Nd(III)], and about 400 μ s in sample f [0.5 wt% Cr(III) and 0.5 wt% Nd(III) in ZBLA glass]. Here the prediction, which is 450 μ s for ZBLA and 337 μ s for PBLA, is near the experimental result, while the short 190 μ s is due to the well-understood cross-relaxation mechanism. A summary of lifetimes of Nd(III) ions in various samples is shown in Tables 4, 5 and 6.

4.3 Cross-relaxation

Special cases of energy transfer are cross-relaxation when the original system loses the energy (E_3-E_2) by obtaining the lower state E_2 (which may also be the ground state E_1) and another system acquires the energy by going to a higher state E_2 . Cross-relaxation may take place between the same lanthanide (being a major mechanism for quenching at higher concentration in a given material) or between two differing elements which happen to have two pairs of energy levels separated by the same amount. The cross-relaxation between a pair of rare earth ions is graphically presented in Fig. 3 of Ref. 46.

The measured lifetime of luminescence is related to the total relaxation rate by

$$1/\tau = \Sigma W_{nr} + \Sigma A + P_{cr} = 1/\tau_0 + P_{cr} \quad (5)$$

where ΣA is the total radiative rate, ΣW_{nr} is the nonradiative rate due to multiphonon relaxation, P_{cr} is the rate of cross-relaxation between adjacent ions, and τ_0 is the intrinsic lifetime.

The critical radius R_0 for cross-relaxation is defined by

$$P_{cr}(R_0) \cdot (1/\tau_0) = 1 \quad (6)$$

R_0 being the critical distance at which the probability for cross-relaxation P_{cr} equals the sum of radiative and multiphonon relaxations.

The cross-relaxation channel for Nd(III) is (${}^4F_{3/2}$) + (${}^4I_{9/2}$) $2({}^4I_{15/2})$. The critical radii in various glasses are presented in Table 7.

TABLE 7. CRITICAL RADII FOR CROSS-RELAXATION OF Nd(III) IN TELLURITE AND FLUORIDE GLASSES

COMPOUND	CONCENTRATION ($10^{20}/\text{cm}^3$)	CRITICAL RADIUS(A)	$\tau_{\text{intrinsic}}$ (μs)	τ_{measured} (μs)	EXCITATION $\lambda(\text{nm})$
0.5/ZnTe	1.10	4.74 ± 0.11	187	178	579
1.6/ZnTe	3.50	5.07 ± 0.36	187	130	579
2.7/ZnTe	5.80	5.81 ± 0.25	187	102	579
0.5/ZBLA	0.85	3.72 ± 0.80	455	443	576
2.0/PBLA	4.02	5.07 ± 0.61	345	264	576
ZnTe--35ZnO, 65TeO ₂					

The lifetimes of emissions originating from ${}^4D_{3/2}$ and from ${}^2P_{3/2}$ are unaffected by the presence of Mn(II) ions for both concentrations of Nd(III) ions. The intensities are much lower, however, in the presence of Mn(II) ions due to radiative loss to Mn(II).

The emission from ${}^4F_{3/2}$ of Nd(III), both in ZBLA and PBLA glass, depends upon whether the emission is measured under excitation at 579 nm directly of Nd(III) or via Mn(II) around 400 nm. Figure 4 presents lifetimes of Nd(III) at various excitations in PBLA glass and Fig. 5 presents the lifetimes of Nd(III) in ZBLA glass. In both cases, when excited at 579 nm, the lifetime is increased by a factor of 3 in ZBLA [1 wt% Mn(II)] and by a factor of 2 in PBLA [24 mole% Mn(II)].

This effect is less pronounced in the case of sample c since the average transfer rate for this sample is faster than the intrinsic lifetime of Nd(III) (Table 6).

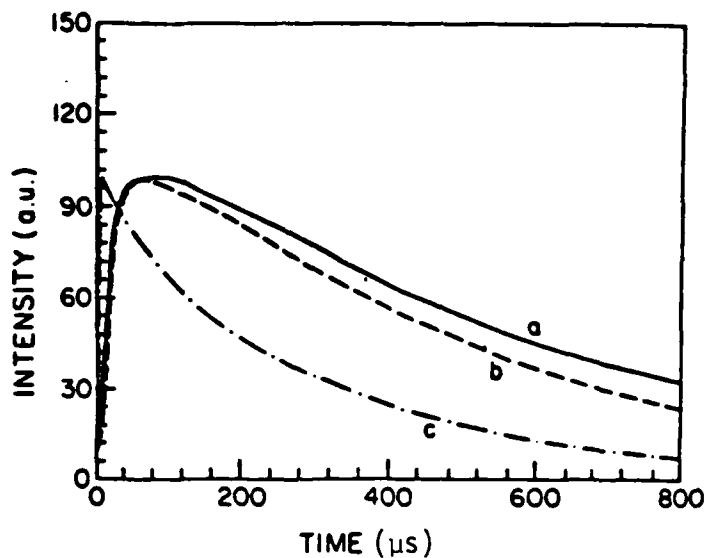


Figure 4. Luminescence decay curves of Nd(III) in PBLA glass ($36\text{PbF}_2, 24\text{MnF}_2, 35\text{GaF}_3, 2\text{AlF}_3, 3.8\text{LaF}_3, 0.2\text{NdF}_3$). (a) Excitation 407 nm. Lifetime 637 μs . Rise time 85 μs . (b) Excitation 337 nm. Lifetime 500 μs . Rise time 70 μs . (c) Excitation 579 nm. Lifetime 330 μs . Rise time 2.0 μs .

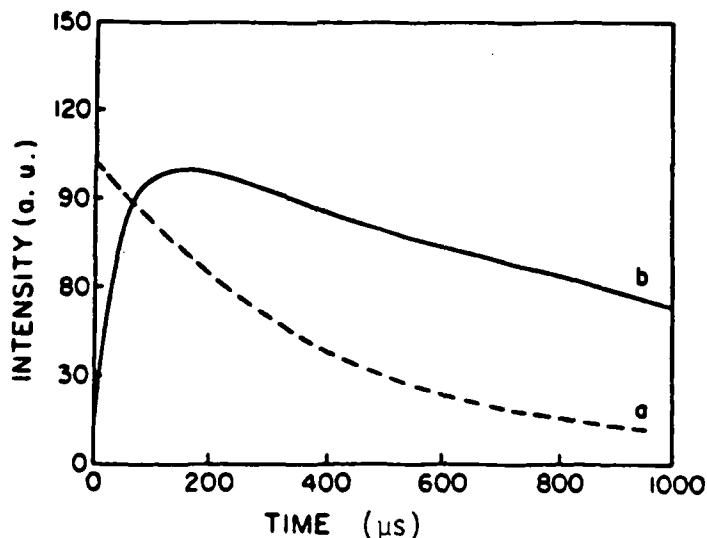


Figure 5. Luminescence decay curves of Nd(III) in ZBLA glass ($55.75\text{ZrF}_4, 33.75\text{BaF}_2, 4.5\text{LaF}_3, 4\text{AlF}_3, 1\text{MnF}_2, 1\text{NdF}_3$). (a) Direct excitation of Nd(III) at 579 nm. Lifetime 340 μs . (b) Excitation of Mn(II) at 404 nm. Lifetime 1450 μs .

In the calculation of radiation transition probabilities, branching ratios and peak cross sections for stimulated emission of rare earths in fluoride glasses, the Judd-Ofelt treatment is applied. This treatment, together with the calculation of the matrix elements of transition, allows prediction of the stimulated cross section which is essential in evaluating laser performance. The formula for peak cross section is (Ref. 48)

$$\sigma = \frac{\lambda^4 A}{8\pi c n^2 \Delta\lambda} \text{ [cm}^2\text{]} \quad (7)$$

where

λ - emission wavelength [cm]

$\Delta\lambda$ - full width at half height of emission band [cm]

n - refractive index

A - radiative transfer probability [s^{-1}]

Threshold power for transverse pumping is

$$P_{th} = \frac{hc(L_0 + L_{res}) \cdot 10^{-7}}{2\lambda_p \tau_f l F \sigma \alpha_p} \quad (8)$$

where L_{res} is resonant power loss due to self-absorption at the laser wavelength, which is defined as

$$L_{res} = 2l\sigma N\beta_y/Z \quad (9)$$

where

N - number density of lasing lines

β_y - Boltzmann factor for the terminal laser level

Z - partition function

l - length of laser

In Nd(III), the terminal level, $^4I_{11/2}$, for the 1060-nm luminescence is positioned at $\approx 2000 \text{ cm}^{-1}$, then $E/kT \approx 10$ at room temperature and the Boltzmann

factor is $\approx 4.5 \times 10^{-5}$. For a 1-cm-long minilaser at representative values of N and σ :

$$L_{\text{res}} \approx 0.2-0.1\%.$$

L_0 - Nonresonant loss which is mainly due to the absorption of the medium and loss at mirrors. It is usually taken to be 0 - 1.5.

λ_p - pumping wavelength. In our case it is 806 nm of LED, having 25-nm bandwidth.

τ_f - lifetime of lasing level.

F - Boltzmann population function of the lasing level. The $^4F_{3/2}$ of Nd(III) is split into 2 main bands in glasses. The fraction of the population at the lasing level (R_1) is 0.64 - 0.72R.

α_p - absorption coefficient of the pumped level, which in our case is centered at 800 nm ($^4F_{3/2} + ^2H_{9/2}$) and is obtained by dividing the optical density of the sample by its thickness.

Table 8 presents the comparison of peak cross-section and threshold power for laser action of Nd(III) in fluoride, oxide and chalcogenide glasses for transverse pumping. The table shows that the laser characteristics for Nd(III) in fluoride glasses are quite similar and even better than in ED-2 glass.

TABLE 8. SPECTROSCOPIC AND LASER PROPERTIES IN FLUORIDE GLASSES AS COMPARED TO OXIDE AND CHALCOGENIDE GLASSES

HOST	ASSIGNMENT	PEAK EMISSION (nm)	CONC. (cm^{-3}) $\times 10^{20}$	ABS. COEF. 806 nm (cm^{-1})	λ (nm)	$\sigma(\text{cm}^2)$ $\times 10^{-20}$	P _{th} (W/cm ²)		τ_f (μs)	REF.
							$L_0=1\%$ $L_r=0.2\%$	$L_0=1\%$ $L_r=0\%$		
ZBLA	$^4F_{3/2}-^4I_{11/2}$	1049	2.72	3.14	26.7	2.9	57	-	400	10
PBLA	$^4F_{3/2}-^4I_{11/2}$	1039	4.02	3.57	33.0	2.75	112	-	190	31
PBLA	$^4F_{3/2}-^4I_{13/2}$	1306	4.02	3.57	65.0	0.85	-	256	190	31
ED-2	$^4F_{3/2}-^4I_{11/2}$	1060	1.83	1.27	27.8	2.9	173	-	300	48
ED-2	$^4F_{3/2}-^4I_{13/2}$	1340	1.83	3.14	64.4	0.72	-	590	300	48
ZnTe	$^4F_{3/2}-^4I_{11/2}$	1060	3.46	4.73	29.0	3.6	93	-	130	31
ZnTe	$^4F_{3/2}-^4I_{11/2}$	1340	3.46	4.73	73.0	0.76	-	367	130	31
GLS	$^4F_{3/2}-^4I_{11/2}$	1077	2.63	14.50	-	7.95	11.3	-	100	47
GLS	$^4F_{3/2}-^4I_{13/2}$	1370	2.63	14.50	-	3.60	-	27.7	100	47
Chalcogenide, GLS - $3\text{Ga}_2\text{S}_3, 0.85\text{LaS}_3, 0.15\text{Nd}_2\text{S}_3$										

5. ENERGY TRANSFER BETWEEN MANGANESE(II) AND NEODYMIUM(III)

The evidence of energy transfer between Mn(II) and Nd(III) has been already given in Chapter 5 when it was shown in Figs. 4 and 5 that Nd(III) can be excited via Mn(II) at 337 nm or at 400 nm. The rise time of about 0.1 ms in Figs. 4 and 5 is characteristic of the time at which the energy transfer takes place. Figure 5 shows the approximately exponential decay with lifetime 0.34 ms by excitation in the Nd(III) band at 579 nm, the emission being measured at 876 nm. When the excitation is done at 404 nm, at the low-energy edge of the narrow $^6S - ^4G$ absorption band of Mn(II), the same Nd(III) emission at 876 nm shows a rise time of about 0.1 ms followed by an exponential decay with the lifetime 1.45 ms. Such storage of energy in the lowest quartet of Mn(II) was previously observed (Ref. 12) for Mn(II) and Er(III) in zinc gallium lead fluoride glass. The energy scheme for transfer between Mn(II) and Nd(III) in such a glass is presented in Fig. 6. In the absence of Nd(III), the luminescence of Mn(II) in ZBLA measured at 545 nm shows an approximately exponential decay curve with lifetime between 13 and 14 ms (note the concentration of Mn(II) of 1 wt%). The simplest rationalization for this

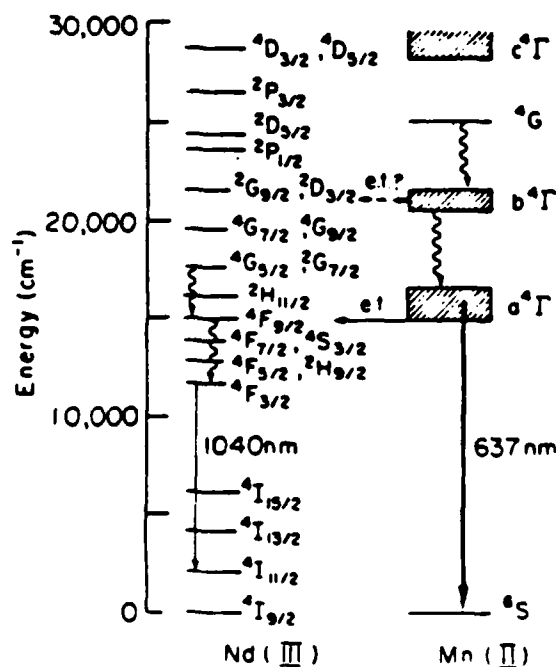


Figure 6. Scheme of energy levels of Nd(III) and Mn(II) in fluoride glass.

decay being 9 times more rapid in the presence of 1 wt% Nd(III) is that the energy transfer is 8 times more rapid under these circumstances than luminescent decay of the Mn(II) quartet state. This mechanism of energy storage has obvious potential applications in laser materials.

The evidence of radiative transfer between Mn(II) and Nd(III) can be seen in Fig. 7 as a dip in the emission spectrum of Mn(II) at a wavelength corresponding to the maximum absorption of Nd(III) (580 nm). Evidence of both radiative and nonradiative energy transfer is found in the excitation spectrum of Nd(III), Fig. 8, where additional bands in the wavelength range 300--520 nm appear.

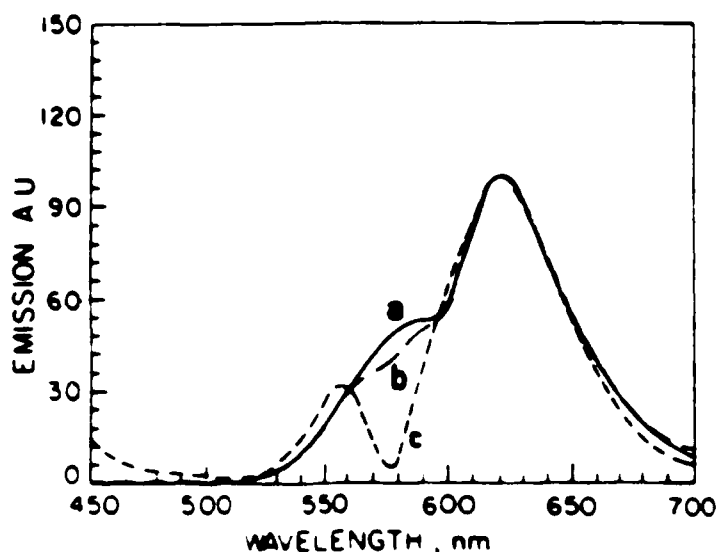


Figure 7. Emission spectrum of Mn(II) in PBLA glass: Excitation at 407 nm. (a) $36\text{PbF}_2, 24\text{MnF}_2, 35\text{GaF}_3, 2\text{AlF}_3, 3\text{YF}_3, 4\text{LaF}_3$. Solid line. (b) $36\text{PbF}_2, 24\text{MnF}_2, 35\text{GaF}_3, 2\text{AlF}_3, 3.8\text{LaF}_3, 0.2\text{NdF}_3$. Enlarged $\times 3$ in respect to (a). (c) $36\text{PbF}_2, 24\text{MnF}_2, 35\text{GaF}_3, 2\text{AlF}_3, 2\text{LaF}_3, 2\text{NdF}_3$. Enlarged $\times 9.8$ in respect to (a). The dip observed around 580 nm is due to absorption by Nd(III).

Mn(II) has one electron in each of the d-like orbitals and thus there is no reason for octahedral symmetry as in Cr(III) where the symmetry is always octahedral by ligand field stabilization (Ref. 49). Thus one can find a variety of compounds in which the coordination number of Mn(II) can acquire values from 4 to 9 (Refs. 12, 50). Mn(II) and Fe(III) have no excited states

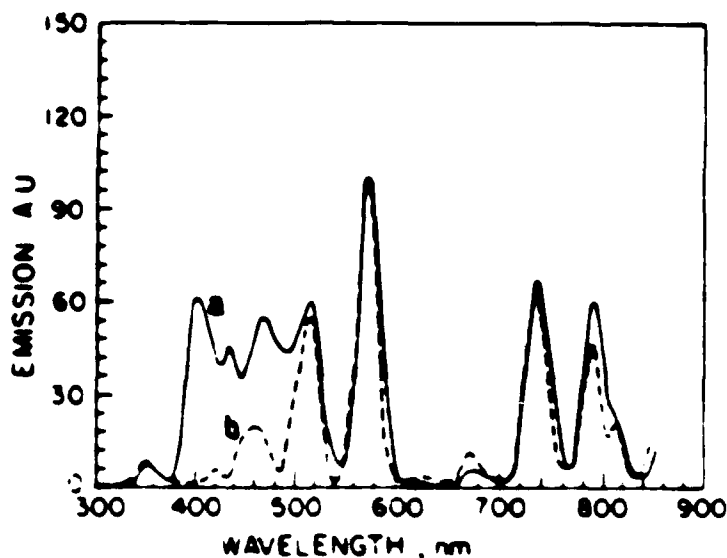


Figure 8. Excitation spectra of Nd(III) in PBLA glass. Uncorrected. Emission at 876 nm: (a) $36\text{PbF}_2, 24\text{MnF}_2, 35\text{GaF}_3, 2\text{AlF}_3, 3.8\text{LaF}_3, 0.2\text{NaF}_3$. (b) $36\text{PbF}_2, 24\text{ZrF}_2, 35\text{GaF}_3, 2\text{AlF}_3, 3\text{YF}_3, 2\text{LaF}_3, 2\text{NaF}_3$.

of the configuration $3d^5$ with the same high total spin quantum number $S = 5/2$ as the sextet ground state 6S ; and among the $252-6=246$ excited states, 96 have $S = 3/2$ (quartets). The first two absorption bands are rather broad, whereas a sharp absorption band situated somewhere in the interval between 25300 and 21100 cm^{-1} corresponds to some of the components of $4G$ lacking ligand field influence. Comparison of this energy difference with 26850 cm^{-1} in gaseous Mn(II) allows a direct evaluation of the nephelauxetic effect indicating weak covalent bonding with the neighbor atoms of the compounds or the glass-forming medium. It is difficult to draw conclusions about the local symmetry of Mn(II) (with the exception of tetrahedral) from the position of the absorption bands below this level. Such conclusions may be drawn to some extent from the emission spectra showing a considerable Stokes shift below the first quartet. For example, salts of the tetrahedral $(\text{MnBr}_4)^{-2}$ show luminescence of the first quartet (Ref. 51) in the green with a quantum efficiency of about 1. On the other hand, the red luminescence of Mn(II) in lanthanum aluminate is ascribed to the octahedrally surrounded Mn(II) by oxygen ions (Ref. 52). Several sites of Mn(II) were observed in calcium fluorophosphate emitting in the red (Ref. 53). In oxide glasses a variety of sites are observed from the different emission spectra (Ref. 50).

The absorption and fluorescence spectra of Mn(II) in phosphate, silicate and borate glasses were treated by "Ligand Field" arguments by Bingham and Parke (Ref. 54). These authors concluded that their silicate glasses have tetrahedral $N = 4$ and phosphate $N = 6$, whereas borate glasses contain a mixture. However, an alternative possibility quite likely to occur also in fluoride glasses is a heterogeneous mixture of several low-symmetry $N = 7$ or 5 and perhaps non-octahedral $N = 6$.

The high quantum yield of Mn(II) luminescence in a variety of glasses (Refs. 49,55) makes them potential materials for luminescent solar concentrators, provided that the low absorption bands arising from the spin-forbidden transitions will be overcome by high concentration of Mn(II). Fortunately, in a number of the glasses the concentration quenching is very low (Ref. 50). Energy transfer from Mn(II) to Nd(III) in calcium phosphate glass and from Mn(II) to Er(III) and to Ho(III) in silicate glass was found to take place by a dipole-dipole interaction (Ref. 56). The same mechanism takes place also in energy transfer between Mn(II) and Nd(III) in barium borate glass (Ref. 57).

Energy transfer between Mn(II) and Er(III) in PBLA glass having composition $36\text{PbF}_2, 24(\text{Mn}, \text{Zn})\text{F}_2, 35\text{CaF}_2, 5\text{Al}(\text{PO}_3\text{F})_3$ doped with Er(III) has been studied recently (Ref. 12). The emission of Mn(II) in absence of Er(III) consists of a broad band centered around 630 nm and an integrated lifetime of 1.4 ms. In the presence of Er(III), the intensity and lifetimes are decreased as a result of energy transfer to the ${}^4\text{F}_9/2$ level of Er(III). The fluorescence of Er(III) arising from ${}^3\text{S}_3/2$ at 543 nm has an integrated lifetime of 60 μs in the absence of Mn(II) and is decreased to 10 μs in the presence of Mn(II) as a result of energy transfer to Mn(II). The 666-nm luminescence of Er(III) is enhanced in the presence of Mn(II) and has a nonexponential time dependence. The longer component corresponds to the transfer of energy from Mn(II) to Er(III), while the short-lived component is probably due to the cascading down Er(III)-Mn(II)-Er(III) through states above the Stokes threshold of Mn(II).

Here we present the results of a study of energy transfer between Mn(II) and Nd(III) ions in two heavy metal fluoride glasses, PBLA and ZBLA.

Since most of the decay curves analyzed in this study are nonexponential, we used the intrinsic lifetime as defined in Eq. 1. We also measured the lifetime at which the intensity decreases to $1/e$ of its initial value (τ_1), to $1/e^2$ (τ_2) and $1/e^3$ (τ_3) of its initial value.

The efficiency of transfer of energy from Mn(II) to Nd(III) was determined both from the time-dependent decay measurements and from the steady-state emission measurements as follows:

$$\eta_{tr}^d = 1 - (\tau_{ina}/\tau_{in}) \quad (10)$$

where τ_{ina} is the integrated lifetime of Mn(II) in the presence of Nd(III) and τ_{in} is the integrated lifetime of Mn(II) without Nd(III) (sample a);

$$\eta_{tr}^s = 1 - \frac{\int I_d^a(\bar{\nu}) d\bar{\nu}}{\int I_d(\bar{\nu}) d\bar{\nu}} \quad (11)$$

where $I_d^a(\bar{\nu})$ is the shape of emission band of Mn(II) in the presence of Nd(III) and $I_d(\bar{\nu})$ is the shape of the emission band in the absence of Nd(III) as a function of energy (cm^{-1}).

The transfer rates of energy transfer were calculated from

$$W_{tr} = 1/\tau_{ina} - 1/\tau_{in} \quad (12)$$

5.1 Manganese - steady state

The emission spectra of samples a, b, and c are shown normalized to the height of the emission spectrum of sample a [24 mole% Mn(II) in PBLA] by factors of 3.8 and 9, respectively, which shows the decrease of the intensity of the emission spectrum with increasing concentration of Nd(III) (Fig. 7). The emission curve of sample c shows a characteristic dip which is ascribed to absorption by the strong ${}^4G_{5/2}$ band of Nd(III) (Ref. 56). This emission band is corrected following reasoning proposed in Ref. 56 prior to integration.

Bands a and b were integrated without correction. The results of calculation of energy transfer efficiencies from these data are shown in Table 9, together with the results obtained from the time-dependent data. The absorption spectrum of sample a containing 24 mole% Mn(II) is shown in Fig. 9. The strong absorption band starting at 290 nm is partly due to Mn(II) and mostly to Pb(II) ions. The sharp maximum at 410 nm is due to a component of 4G manifold lacking ligand field influence. The excitation spectra of sample a [24 mole% Mn(II) in PBLA] and sample g [0.5% Cr(III) + 0.5% Mn(II) in ZBLA] together with the corresponding emission spectra are shown in Fig. 10. Maximum of the emission spectra of sample g occurs at 545 nm, which, according to Bingham and Parke (Ref. 54), is characteristic of tetrahedral symmetry, while the 637-nm emission of sample a indicates preferential octahedral coordination of Mn(II). However, other authors (Ref. 58) point out that the wavelength of emission is a smooth function of concentration of Mn(II), the green emission being common for low concentrations and the red emission for high concentrations of Mn(II). Moreover, the emission wavelength may be also a function of temperature (Ref. 59).

TABLE 9. EFFICIENCY OF ENERGY TRANSFER FROM Mn(II) to Nd(III) IN PBLA GLASS $35\text{PbF}_2, 24\text{MnF}_2, 35\text{GaF}_3, \text{AlF}_3, (4-x)\text{LaF}_3, x\text{NdF}_3$

X	EXCITATION WAVELENGTH	EFFICIENCY FROM		TRANSFER RATE (s^{-1})
		DECAY TIME	STEADY STATE	
0.2	407	0.52	0.57	1040
0.2	337	0.57	0.56	1550
2.0	407	0.94	0.93	14400
2.0	337	0.92	0.92	12700

5.2 Manganese lifetimes

The decay curves of luminescence of Mn(II) in samples a, b, and c are in general nonexponential. Examination of Tables 10 and 11 and Fig. 11 reveals some of the general features of Mn(II) luminescence in our samples: (a) The measured lifetime of Mn(II) in sample a ($35\text{PbF}_2, 24\text{MnF}_2, 35\text{GaF}_3, 2\text{AlF}_3, 3\text{YF}_3, 4\text{LaF}_3$) is of the order of 1 ms as compared with ≈ 14 ms in diluted samples, which

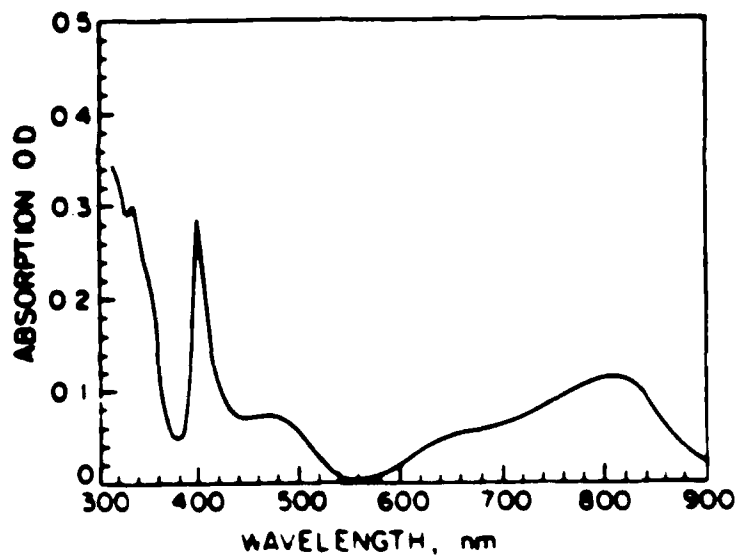


Figure 9. Absorption spectrum of Mn(II) in PBLA glass
36PbF₂, 24MnF₂, 35GaF₃, 2AlF₃, 3YF₃, 4LaF₃.

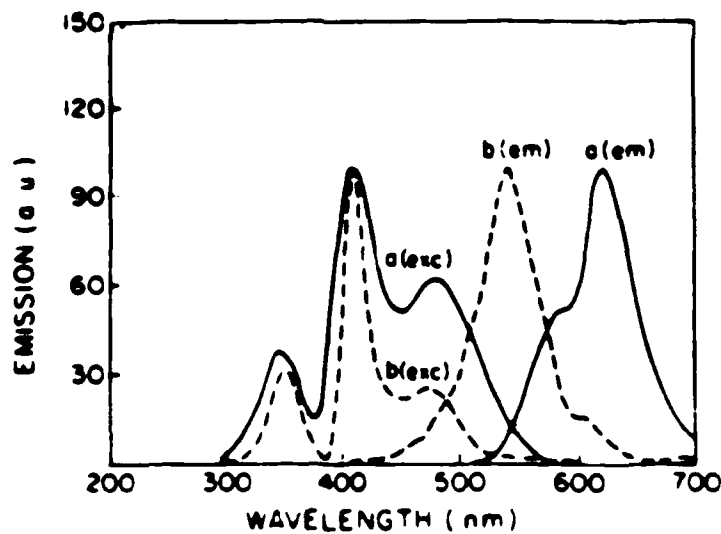


Figure 10. Excitation and emission spectra of Mn(II) in PBLA and ZBLA glasses: (a) 36PbF₂, 24MnF₂, 35GaF₃, 2AlF₃, 3YF₃, 4LaF₃. Emission spectrum excited at 407nm
(b) 55.75AlF₄, 33.75BaF₂, 4.5LaF₃, 4AlF₃, 1MnF₂, 1NaF₃. Emission spectrum excited at 407 nm.

Indicates that in this system the interactions among the Mn(II) ions are strong and the ions undergo concentration quenching. (b) The lifetime of Mn(II) ions depends both on concentrations of ions of Nd(III) and on the wavelength of the excitation. The initial part of each decay curve consists of two components: the fast rise reaching its maximum at 0.5--0.6 μ s and the slow rise reaching its maximum at 1--3 μ s, depending on the wavelength of excitation and concentration of Nd(III) ions. The varying degree of the slow rise time indicates a complicated interaction among the emitting levels of Mn(II) and the Nd(III) levels pumped from them.

These features, however, are within the general trend of decreasing lifetime of Mn(II), with increasing concentration of Nd(III) ions.

TABLE 10. LIFETIMES OF Mn(II) IN ZBLA GLASS

MOLE% OF:		WAVELENGTH (nm)		LIFETIMES (ms)			
DOPANT	Mn(II)	EXCITATION	EMISSION	τ_1	τ_2	τ_3	τ_{in}
1.0 Nd(III)	1.0	337	545	7.4	10.0	11.4	10.4
1.0 Nd(III)	1.0	400	545	12.0	12.4	12.5	12.5
1.0 Nd(III)	1.0	414	545	9.0	10.9	14.4	12.5
0.5 Cr(III)	0.5	337	545	11.7	13.7	14.7	14.0
0.5 Cr(III)	0.5	400	545	12.1	13.7	13.9	13.7
0.5 Cr(III)	1.0	450	545	12.0	13.0	14.0	13.7

TABLE 11. LIFETIMES OF Mn(II) IN PBLA GLASS:

35PbF₂, 24MnF₂, 35GaF₃, 2AlF₃, (4-x)LaF₃, xNdF₃

X	WAVELENGTH (nm)		LIFETIMES (μ s)				RISETIME	
	EXCITATION	EMISSION	τ_1	τ_2	τ_3	τ_{in}	SHORT	LONG
0.0	407	637	905	1040	1040	1040	0.6	3.0
0.0	337	637	676	820	922	870	0.6	1.5
0.0	460	637	512	800	1126	910	0.6	2.5
0.2	407	637	425	510	685	510	0.5	2.0
0.2	337	637	350	385	390	370	0.5	1.5
2.0	414	637	27	55	76	65	<0.5	1.0
2.0	337	637	60	70	85	72	<0.5	1.0

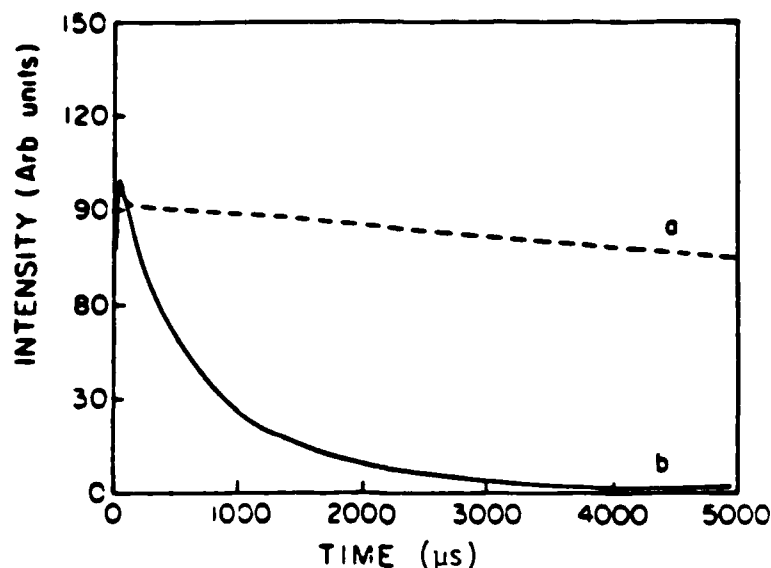


Figure 11. Luminescent decay curves of Mn(II) in PBLA and ZBLA glasses: (a) $56.50\text{ZrF}_4, 34.00\text{BaF}_2, 4.5\text{LaF}_3, 4\text{AlF}_3, 0.5\text{CrF}_3, 0.5\text{MnF}_2$. Excitation at 407 nm, emission at 545 nm, lifetime 14 ms. (b) $36\text{PbF}_2, 24\text{MnF}_2, 35\text{GaF}_3, 2\text{AlF}_3, 3\text{YF}_3, 4\text{LaF}_3$. Excitation at 407 nm, emission at 637 nm, lifetime 1.04 ms.

The efficiency of energy transfer from Mn(II) to Nd(III) is calculated in Eq. 10 and compared with results obtained from steady-state data.

A fair agreement between the two series of results indicates that the two methods are mutually consistent in respect to the system studied. Average energy transfer rates are calculated from Eq. 12 and shown in Table 9.

The efficiency of energy transfer in ZBLA glass was calculated assuming that the lifetime of Mn(II) in sample g [0.5 mole% Mn(II), 0.5 mole% Cr(III)] equals the lifetime of Mn(II) only (which was not available). Then the transfer rate is $1/12.5 - 1/14 = 8.5 \text{ s}^{-1}$ using Eq. 12.

Further examination of the tables leads to a suggestion that the transfer rate depends, to some extent, on the wavelength of excitation, since both the rise time and lifetime of $^4\text{F}_{3/2}$ are shorter when excited through 337 nm than when excited through 414 nm of Mn(II). The phenomena may be ascribed to a greater part of the emission originating from the direct excitation rather

than from the energy transfer; however, the lifetime of Mn(II) in sample b is also shortened considerably when excited with 337 nm of nitrogen laser, indicating that in this case the energy transfer is faster.

The emission labeled with question mark instead of assignment and placed at 810--820 nm was observed both in steady-state emission measurement as a small bump near the shoulder of the emission from ${}^4F_{3/2}$ and in time-dependent measurements. The emission belongs, in respect to its energy, to ${}^4F_{5/2} - {}^4I_{9/2}$. Its lifetime in sample d (2 mole% Nd(III) only) is too short to be measured by our apparatus which also conforms to the predicted lifetime, which is ≈ 10 ns. However, the presence of Mn(II) enhances its luminescence a great deal, as can be seen in the tables. Its lifetime in Mn(II) doped samples is of the order of hundreds of microseconds and its rise time is long. The presence of Mn(II) induces the energy transfer at levels higher than the ${}^4F_{5/2}$ state, and the transfer rate which is the slower process is the bottleneck which determines the reaction rate (Ref. 62). The similar experimental phenomena at which emission from ${}^4F_{5/2}$ could be observed in a CsMnBr₃ crystal doped with traces of Nd(III) ions has been reported (Ref. 60). Lifetimes were not measured in the experiment, however.

6. DISCUSSION

The transfer rates as calculated from the experimental data indicate that the rates proceed roughly according to first-order kinetics, the concentration of Mn(II) being constant and concentration of Nd(III) being variable in our system. On the other hand, the transfer rates depend strongly on the concentration of Mn(II) as follows from the comparison of transfer rates found for 24 mole% Mn(II) in PBLA glass and for 1% Mn(II) in ZBLA glass. The conclusion being in full accord with intuition nevertheless raises the question whether the kinetics depend on the concentration of ground state Mn(II) ions or the excited ions. In our work we observed a systematic trend of faster transfer rates and shorter lifetimes of Mn(II) in the presence of Nd(III) when the samples were excited at 337 nm. The intensity of the 337-nm light from the nitrogen laser is, in our case, a factor of 10 higher than the 407-nm light from a dye laser, and the oscillator strength of Mn(II) at 337 nm is some 5 times lower than at 407 nm. Thus we can expect a twofold increase in excited Mn(II) concentration in the case of excitation at 337 nm. If the transfer rates were dependent on the concentration of the excited Mn(II) ions, we would then expect an increase in transfer rate, decrease in the lifetime of Mn(II), decrease in the rise time of decay of Nd(III) $^4F_{3/2}$ level, and decrease in the lifetime of the same level. Our results conform quantitatively to the prediction.

7. REVIEW

Energy transfer between manganese and neodymium ions in the system studied proceeds through at least three distinct channels:

(1) Radiative energy transfer from neodymium to manganese ions in the range of 27700 cm^{-1} to 22000 cm^{-1} .

(2) Nonradiative energy transfer from manganese to neodymium ions. The energy transfer occurs probably among the lowest manifold of manganese and a number of levels of neodymium in the range of 25000 cm^{-1} to 20000 cm^{-1} .

The transfer rate of the process is almost linear with concentration of neodymium ions, from 0.2 mole% of neodymium to 2.0 mole% at constant 24 mole% of manganese. At low concentration of neodymium the manganese serves as an efficient storage of energy, which results in the lifetime of neodymium with a factor of 2 longer than its intrinsic lifetime. The phenomena may be utilized in a Q-switched Nd laser for energy storage.

(3) Radiative energy transfer from manganese to neodymium ions. The radiation emitted by manganese is absorbed by the ${}^4G_{5/2}$ band in the region around 600 nm.

There is evidence pointing towards the role the intensity of the exciting light plays in respect to the rate of energy transfer between Mn(II) and Nd(III) in the system investigated.

A series of experiments is planned in order to study the dependence of the energy transfer rate on the intensity of exciting light, as well as a number of computer simulations of the appropriate model.

The systems studied are particularly suitable for a theoretical analysis; the PBLA samples represent an almost ideal case of acceptors Nd(III) which do not interact strongly (sample b), and a similar case with a moderately strong interaction among the acceptors (sample c).

On the other hand, the sample h in the ZBLA glass represents a system in which there is a moderate interaction between the donors and weak interaction between the acceptors at equal concentrations of both. Finally, by examining Table 8 we concluded that Nd(III) in fluoride glasses has good laser qualities and could be incorporated into fiber optics systems as an integrated light source.

8. RECOMMENDATIONS

Plans are to extend our study to a new type of fluoride glasses based on heavy metals doped with Ho(III) and Er(III) in order to calculate the laser properties of these glasses. We also recommend that the study on energy transfer between Mn(II) and Nd(III) in ZBLA glasses be extended to a variety of concentrations of Nd(III) and Mn(II) in order to determine the optimum conditions for lasing in these glasses.

REFERENCES

1. Poulain, M., Poulain, M. and Lucas, J., Mater. Res. Bull. 10, 243 (1975).
2. Poulain, M., Chanthanasinh, M. and Lucas, J., Mater. Res. Bull. 12, 151 (1977).
3. Poulain, M. and Lucas, J., Verres Refract. 32, 505 (1978).
4. Miranday, J. P., Jacoboni, C. and De Pape, R., J. Noncryst. Solids 43, 393 (1981).
5. Miranday, J. P., Jacoboni, C. and De Pape, R., Rev. Chim. Miner. 16, 277 (1979).
6. Tran, D. C., Sigel, G. H., Jr. and Bendow, B., J. Lightwave Technology, LT-2, 566 (1984).
7. Drexhage, M. G., Moynihan, C. T., Saleh Boulos, M. and Quinlan, K. P., Proc. Conf. Phys. Fiber Optics (B. Bendow and S. S. Mitra, Eds.), Amer. Ceramic Soc., Columbus, Ohio (1981).
8. Bendow, B., Brown, R. N., Drexhage, M. G., Loretz, T. J. and Kirt, R. L., Appl. Opt. 20, 3688 (1981).
9. Bendow, B., Drexhage M. G. and Lipson, H. G., J. Appl. Phys. 52, 1460 (1981).
10. Lucas, J., Chanthanasinh, M., Poulain, M., Poulain, M., Brun, P. and Weber, M. J., J. Noncryst. Solids 27, 273, (1978).
11. Lucas, J., J. Less-Common Metals 112, 27 (1975).
12. Reisfeld, R., Greenberg, E., Jacoboni, C., De Pape, R. and Jorgensen, C. K., J. Solid State Chem. 53, 236 (1984).
13. Eyal, M., Greenberg, E., Reisfeld, R. and Spector, N., Chem. Phys. Lett. 117, 108 (1985).
14. Adam, J. L. and Sibley, W. A., J. Noncryst. Solids 76, 267 (1985).
15. Blanzat, B., Boehm, L., Jorgensen, C. K., Reisfeld, R. and Spector, N., J. Solid State Chem. 32, 185 (1980).
16. Reisfeld, R., Greenberg, E., Brown, R. N., Drexhage, M. G. and Jorgensen, C. K., Chem. Phys. Lett. 95, 91 (1983).
17. Tanimura, K., Shinn, M. D., Sibley, W. A., Drexhage, M. G. and Brown, R. N., Phys. Rev. B 30, 2429 (1984).
18. Reisfeld, R., Eyal, M., Greenberg, E. and Jorgensen, C. K., Chem. Phys. Lett. 118, 25 (1985).

REFERENCES (Continued)

19. Reisfeld, R., Katz, G., Spector, N., Jorgensen, C. K., Jacoboni, C. and De Pape, R., J. Solid State Chem. 41, 253 (1982).
20. Reisfeld, R., Katz, G., Jacoboni, C., De Pape, R., Drexhage, M. G., Brown, R. N. and Jorgensen, C. K., J. Solid State Chem. 48, 323 (1983).
21. Shinn, M. D., Sibley, W. A., Drexhage, M. G. and Brown, R. N., Phys. Rev. B. 27, 6635 (1983).
22. Ohishi, Y., Mitachi, S., Kanamori, K. and Manabe, T., Phys. Chem. Glasses 24, 135 (1983).
23. Reisfeld, R., Proc. Int'l. Symp. on Rare Earth Spectroscopy, Wroclaw, Poland, 1984; World Scientific Pub. Co. PTE. Ltd. 587 (1985).
24. Bendow, B., Banerjee, P. K., Lucas, J., Fonteneau, G. and Drexhage, M. G., J. Am. Ceramic Soc., 68, C92 (1985).
25. Jorgensen, C. K., Oxidation Numbers and Oxidation States, Springer-Verlag, Berlin (1969).
26. Jorgensen, C. K., Modern Aspects of Ligand Field Theory, North-Holland, Amsterdam (1971).
27. Jorgensen, C. K., Pappalardo, R. and Ritterhaus, E., Z. Naturforsch. 20a, 54 (1965).
28. Reisfeld, R., Rep. Ser. Swedish Acad. Engineering Sciences in Finland, (Proc. Advanced Summer School on Electronic Structure of New Materials, Loviisa, Finland, 1984) 40, part I, 7 (1985).
29. Ferguson, J., Guggenheim, H. J. and Wood, D. L., J. Chem. Phys. 54, 504 (1971).
30. Andrews, L. J., Lempicki, A. and McCollum, B. C., J. Chem. Phys. 74, 5526 (1981).
31. Reisfeld, R., Eyal, M., Jorgensen, C. K., Guenther, A. H. and Bendow, B., Chimia (in publication).
32. Reisfeld, R., and Kisilev, A., Chem. Phys. Lett. 115, 457 (1985).
33. Reisfeld, R., Kisilev, A., Greenberg, E., Buch, A. and Ish-Shalom, M., Chem. Phys. Lett. 104, 153 (1984).
34. Kisilev, A., Reisfeld, R., Greenberg, E., Buch, A. and Ish-Shalom, M., Chem. Phys. Lett. 105, 405 (1984).
35. Bouderbala, M., Boulon, G., Reisfeld, R., Buch, A., Ish-Shalom, M. and Lejus, A. M., Chem. Phys. Lett. 121, 535 (1985).

REFERENCES (Continued)

36. Kisilev, A., and Reisfeld, R., Solar Energy 33, 163 (1984).
37. Rudorff, W., Kandler, J. and Babel, D., Z. Anorg. Chem. 317, 261 (1962).
38. Smith, D. W., J. Chem. Phys. 50, 2784 (1969).
39. Hitchman, M. A. and Waite, T. D., Inorg. Chem. 15, 2150 (1976).
40. Urland, W., Chem Phys. Lett. 83, 116 (1981).
41. Gerlock, M. and Woolley, R. G., Progress Inorg. Chem. 31, 371 (1984).
42. Cramer, S. P. and Hodgson, K. O., Inorg. Chem. 25, 1 (1979).
43. Reisfeld, R. and Jorgensen, C. K., Lasers and Excited States of Rare Earths, Springer-Verlag, Berlin (1977).
44. Nielson, C. W. and Koster, G. F., Spectroscopic Coefficients for the p_n , d_n and f_n Configurations, MIT Press, Cambridge, (1964).
45. Weber, M. J., Proc. Int'l. Conf. on Lasers '82, New Orleans, Dec. 13--17 (1982).
46. Reisfeld, R. and Eyal, M., J. de Physique, Colloque 7, 349 (1985).
47. Bornstein, A. and Reisfeld, R., J. Noncryst. Solids 50, 23 (1982).
48. Stokowski, S. E. and Weber, M. J., Laser Glass Handbook M-95, Lawrence Livermore National Laboratory, California (1979).
49. Reisfeld, R. and Jorgensen, C. K., Structure and Bonding 49, 1 (1982).
50. Reisfeld, R., Kisilev, A. and Jorgensen, C. K., Chem. Phys. Lett. 111, 19 (1985).
51. Jorgensen, C. K., Acta Chem. Scand. 11, 53 (1957).
52. Stevels, A. L. N., J. Luminescence 20, 99 (1979).
53. Ryan, F. M., Ohlmann, R. C., Murphy, J., Mazelsky, R., Wagner, G. R. and Warren, R. W., Phys. Rev. B 2, 2341 (1970).
54. Bingham, K. and Parke, S., Phys. Chem. Glasses 6, 224 (1965).
55. Kisilev, A., Reisfeld, R. and Tzeheval, H., 4th Int'l Conf. on Photochem. Conversion and Storage of Solar Energy, Book of Abstracts, 299 (1982).
56. Parke, S. and Cole, E., Phys. Chem. Glasses 12, 123 (1971).
57. Kumar, R., Chem. Phys. Lett. 45, 121 (1977).

REFERENCES (Concluded)

58. Turner, W. H. and Turner, J. E., J. Am. Chem. Soc. 53, 329 (1970).
59. Linwood, S. H. and Weil, W. A., J. Am. Opt. Soc. 32, 443, (1942).
60. McPherson, G. and Francis, A. H., Phys. Rev. Lett. 41, 1681, (1978).
61. Reisfeld, R., J. Less-Common Metals, 112, 9 (1985).
62. Eyal, M., "Glass Lasers and Solar Applications," Spectroscopy of Solid State Laser-Type Materials, ed. B. DiBartolo, Plenum Press, New York, New York (1987).

END

8-87

DTIC